

## **CHAPTER 2**

# **SWASH MOTION DUE TO OBLIQUELY INCIDENT WAVES**

**Toshiyuki Asano<sup>1</sup>**

### **abstract**

A numerical model is developed to predict the flow characteristics in a swash zone for obliquely incident wave trains. The two-dimensional shallow water equations are de-coupled into independent equations each for on-off shore motion and for longshore motion. A front of swash wave train is treated as a moving boundary which makes the solution predictable for landward zone of the still water level. The results show non-vanishing longshore velocities and volume flux at the still water shoreline. These quantities are found to increase with the beach slope. The two-dimensional uprush and downrush motion near the front of swash waves shows skew figures, which may cause zig-zag longshore sediment transport inherent in swash zone.

### **1.INTRODUCTION**

Swash zone is the most familiar area that we can easily observe its motion while walking along a sandy beach, but it is one of the unsolved area from the hydrodynamic point of view. The difficulty lies on that waves in swash zone are highly nonlinear and show such a unique behaviour that the seabed is immersed during run-up and dried during run-down alternatively. Lately, the swash motion has received much attention because the sediment process in this zone provides the important boundary condition for the beach evolution. And also, recent studies have reported an important new finding that longshore sediment transport takes two major peaks located at the breaking point and on the foreshore in the swash zone(Bodge - Dean, 1987; Kamphuis, 1991;b).

Under obliquely incident waves, sediment near shoreline moves in a zig-zag way which results in the inherent longshore transport in the swash zone.

---

<sup>1</sup>Dept. of Ocean Civil Engrg., Kagoshima Univ., Korimoto, Kagoshima, 890, JAPAN

Intensive turbulence generated in the uprush and backwash waves causes a large volume of sediment to be suspended. Moreover, infragravity wave motion might be more influential on the sediment dynamics in this very shallow water region (Thornton - Abdelrahman, 1991).

Although such complicated dynamics needs to be investigated for full descriptions, this study, as the first step, focuses on the velocity field as a basic forcing function of the sediment motion under obliquely incident monochromatic waves. The horizontally two-dimensional water particle velocities are computed based on Ryrie(1983)'s analysis. Moreover, the velocity measurements in the swash zone under obliquely incident waves are conducted using tracer method. Through comparisons between the numerical and experimental results, the hydrodynamic properties related to longshore sediment transport are discussed.

## 2. NUMERICAL ANALYSIS

### 2.1 Formulation of Shallow Water Wave Equations

Based on Ryrie's formulation, the following two dimensional wave and topographic system is assumed. The incident monochromatic waves with straight parallel crests are assumed to arrive at the seaward boundary with an angle  $\theta_B$  (Fig. 1). The  $x'$  - and  $y'$  - axis, in which the prime indicates the dimensional variables, is chosen to be in the normal and the parallel direction to the shoreline, respectively. The  $z'$  - axis is taken positive upward with  $z' = 0$  at the still water level(SWL). The beach slope  $S'$  is herein restricted to be uniform and its contours are assumed to be straight and parallel to the shoreline. The water depth at the toe of the slope is given as  $d'_B$  where the offshore boundary conditions for the incident waves are provided. The free surface is located at  $z' = \eta'$ , so that the instantaneous water depth  $h'$  is given by  $h' = \eta' + (d'_B - S'x')$ .

The governing equations for the mass and momentum conservations may be expressed as

$$\frac{\partial h'}{\partial t'} + \frac{\partial}{\partial x'}(h'u') + \frac{\partial}{\partial y'}(h'v') = 0 \quad (1)$$

$$\begin{aligned} \frac{\partial}{\partial t'}(h'u') + \frac{\partial}{\partial x'}(h'u'^2) + \frac{\partial}{\partial y'}(h'u'v') = \\ -gh'\frac{\partial\eta'}{\partial x'} - \frac{1}{2}f' | u' | u' \end{aligned} \quad (2)$$

$$\begin{aligned} \frac{\partial}{\partial t'}(h'v') + \frac{\partial}{\partial x'}(h'u'v') + \frac{\partial}{\partial y'}(h'v'^2) = \\ -gh'\frac{\partial\eta'}{\partial y'} - \frac{1}{2}f' | u' | v' \end{aligned} \quad (3)$$

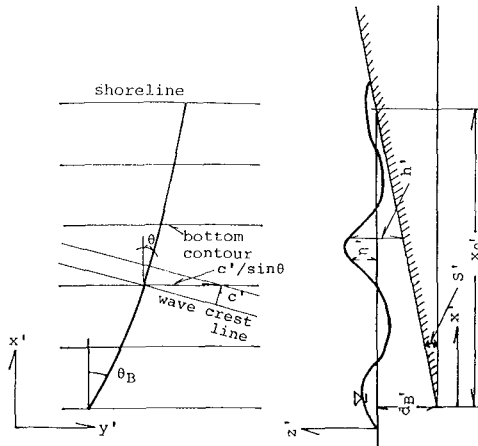


Fig. 1: Two dimensional plane wave on a uniform beach

in which,  $t'$  is the time,  $u'$ ,  $v'$  is the on-offshore and longshore velocity respectively,  $g$  is the gravitational acceleration and  $f'$  is the bottom friction factor. Eqs.(2) and (3) are the two dimensional nonlinear shallow water equations, where the vertical pressure distribution is assumed to be hydrostatic.

According to Kobayashi et al.(1987), the following dimensionless variables using the characteristic period  $T'$  and height  $H'$  associated with the incident wave train are introduced.

$$\begin{aligned} u &= \frac{u'}{\sqrt{gH'}}; \quad \eta = \frac{\eta'}{H'}; \quad h = \frac{h'}{H'}; \quad t = \frac{t'}{T'}; \\ x &= \frac{x'}{T'\sqrt{gH'}}; \quad c = \frac{c'}{\sqrt{gH'}}; \quad f = \frac{1}{2}\sigma f'; \\ S &= T'\sqrt{\frac{g}{H'}}S'; \quad d_B = d'_B/H'; \quad \sigma = T'\sqrt{g/H'}; \end{aligned} \quad (4)$$

in which,  $S$  is expressed by the surf similarity parameter  $\xi$  as  $S = \sqrt{2\pi}\xi$ ,  $d_B$  corresponds to the inverse number of relative water depth at the offshore boundary and  $\sigma/h$  means the ratio of wave length to water depth  $L'/h'$ .

Since we have assumed that the wave crest is straight parallel and bottom topography does not vary in the  $y$ -direction, the observed wave motion moving along the longshore direction at the speed  $C'/\sin\theta$  (which remains constant throughout the surf zone by Snell's law) becomes independent in the  $y$ -direction. Consequently, a new independent variable referred to "pseudotime"  $\hat{t}'$  is introduced to unify two independent variables  $t'$  and  $y'$ .

$$\hat{t}' = t' - \frac{\sin\theta_B}{C'_B}y' \quad (5)$$

Providing the incident wave angle  $\theta_B$  is small, the following small parameter  $\epsilon$  can be used for the scaling of the governing equations

$$\epsilon = \frac{\sin \theta_B}{C'_B} \sqrt{g H'} \quad (6)$$

Since the length scale of variations in the  $y'$  direction is much greater than that in the  $x'$  direction and also the velocity  $v'$  is much smaller than  $u'$ , we introduce the following transformations in order to make these variables of order unity

$$v = \frac{v'}{\epsilon \sqrt{g H'}}; \quad y = \frac{\epsilon y'}{T' \sqrt{g H'}} \quad (7)$$

Using the above scaling parameters and transformations, the normalized pseudotime is given by,

$$\hat{t} = t - y \quad (8)$$

and the differentiations with the dimensional variables are replaced by as follows.

$$\frac{\partial}{\partial t} = \frac{\partial}{\partial \hat{t}} \quad \frac{\partial}{\partial y} = -\frac{\partial}{\partial \hat{t}} \quad (9)$$

After these deductions, the original equations (1) ~ (3) are considerably simplified into the following non-dimensional form.

$$\frac{\partial h}{\partial \hat{t}} + \frac{\partial(uh)}{\partial x} = \epsilon^2 \frac{\partial(vh)}{\partial \hat{t}} \quad (10)$$

$$\frac{\partial u}{\partial \hat{t}} + u \frac{\partial u}{\partial x} + \frac{\partial h}{\partial x} + S + \frac{f u |u|}{h} = \epsilon^2 v \frac{\partial u}{\partial \hat{t}} \quad (11)$$

$$\epsilon \left\{ \frac{\partial v}{\partial \hat{t}} + u \frac{\partial v}{\partial x} - \frac{\partial h}{\partial \hat{t}} + \frac{f |u| v}{h} \right\} = \epsilon^3 v \frac{\partial v}{\partial \hat{t}} \quad (12)$$

If we neglect higher terms than  $O(\epsilon^2)$ , that is, the right hand sides of Eqs. (10), (11) are set to be zero, the resultant equations are the same as the usual one dimensional shallow water wave equations normally incident to the shoreline. If we consider Eq. (12) in the order  $O(\epsilon)$ , the equation becomes as

$$\frac{\partial v}{\partial \hat{t}} + u \frac{\partial v}{\partial x} - \frac{\partial h}{\partial \hat{t}} + \frac{f |u| v}{h} = 0 \quad (13)$$

After all, the leading order in  $\epsilon$  of perturbation equations yields decoupled equations each for on-offshore motion and for longshore motion. Thus, the longshore velocity  $v(x, \hat{t})$  can be solved like one-dimensional analysis once  $h(x, \hat{t})$  and  $u(x, \hat{t})$  is known.

## 2.2 Numerical Method

The basic equations were solved using an explicit Lax-Wendroff finite difference method. To attenuate numerical oscillations in the vicinity of wave front, a so-called artificial-viscosity term was included (Hibberd-Peregrine, 1979). The computational domain in the cross shore direction was discretized into 100 grid points so that one wave length can be represented at least 20 grid points. The time discretization was set as  $\Delta t = T/4000$ .

The initial condition for free water surface  $\eta$  is still water condition;  $\eta = 0$ . Accordingly, the flow velocities  $u$  and  $v$  are set to be zero for all the computational domain. The offshore boundary was set at around one wave length offshore from the breaking point so that the boundary value for time averaged longshore velocity  $V$  may be given by zero. The offshore boundary should be devised to make the reflected waves from the on-shore side transmit through the boundary freely. The total water depth at the offshore boundary is expressed as

$$h_B = d_B + \eta_i(t) + \eta_r(t), \quad \text{at } x = 0 \quad (14)$$

in which,  $\eta_i$ ,  $\eta_r$  denotes the water surface fluctuation due to the incident and reflected waves, respectively. The time variation  $\eta_r$  was evaluated using the retreat characteristic variable  $\beta$  as follows (Kobayashi et al., 1987)

$$\eta_r(t) = \sqrt{d_B \beta(t)/2} - d_B, \quad \text{at } x = 0 \quad (15)$$

The offshore boundary condition for  $u_B$  is easily determined by the boundary values of  $\beta$  and  $h_B$ , and that for  $v_B$  was assumed to be  $u_B \tan \theta$ . The onshore boundary was treated as a moving boundary in which the front of wet waterline node was determined as such a location that the total water depth is less than a given threshold small depth (Hibbert-Peregrine, 1979).

## 2.3 Numerical Results

Calculations were carried out under similar conditions of Kamphuis's experiments(1991; a, b); that is , the water depth at the offshore boundary  $d'_B = 0.50\text{m}$ , the incident wave height  $H' = 12.4\text{cm}$ , wave period  $T' = 1.15\text{s}$ , incident wave angle  $\theta_B = 10^\circ$ , beach slope  $S' = 1/10$ .

Fig. 2 shows the computed spatial variations of free surface elevation  $\eta'$  (bottom), on-offshore velocity  $u'$  (middle) and longshore velocity  $v'$  (top). Fig. 2(a) and (b) shows the results under the bottom friction factor  $f' = 0.01$  and  $f' = 0.10$ , respectively. Comparison of these figures indicates that the results of free surface elevation  $\eta'$  and on-offshore velocity  $u'$  are little affected by the change of the friction factor, whereas the results of the longshore velocity  $v'$  shows the considerable difference by  $f'$  especially around the still water shoreline(S.W.S.L.).

Fig. 2(c) and (d) are the results when the beach slope  $S'$  is changed from the original input condition. Although, Eq. (13) for the longshore velocity  $v'$  does not include  $S'$  term, the effects of beach slope are indirectly involved in  $v'$

through the alterations of  $h'$  and  $v'$  by  $S'$ . Under the mild slope case  $S' = 1/20$ , the longshore velocity around S.W.S.L. takes small value as shown in Fig. 2(c). On the other hand, under steep slope case  $S' = 1/5$ , the longshore current velocity becomes large even in the landward region of S.W.S.L. The longshore velocity  $v'$  near S.W.S.L. is found to be positive not only up-rush phase but also down rush phase.

In order to discuss the properties of calculated longshore velocity, the following characteristics are investigated; the peak value of temporal velocity fluctuation at a specific point;  $v'_{peak}$ , the time average value;  $v'_{mean}$  and the volume flux of longshore velocity;  $Q'$ , defined as

$$Q' = \frac{1}{T} \int_0^T h' v' dt \quad (16)$$

Fig. 3 illustrates the on-offshore variations of the above characteristics. As the beach slope  $S'$  becomes steeper, all the characteristics increase and the peaks of the distributions move toward S.W.S.L. (Fig. 3(a)). Non-vanishing velocities and volume flux are found at the still water shoreline and in further landward region. Fig. 3(b) indicates the effect of incident wave period  $T'$ , where the increase of  $T'$  has the same effects as the increase of  $S'$ . Fig. 3 (c) illustrates the results when the friction factor  $f'$  is varied. The characteristics decrease with the friction factor, but the differences are not so significant.

Fig. 4 shows the temporal variations of free surface elevation  $\eta'$  (bottom), velocity vector  $v'$  (middle) and volume flux vector  $Q'$  (top) at the locations from offshore to onshore. In order to stress the difference between run-up and downwash motion, this calculation was carried out under relatively steep slope  $S' = 1/5$  and large wave incident angle  $\theta_B = 20^\circ$ . The stick-diagrams of  $v'$  show that the water mass runs up on the beach with a certain angle to the shoreline, then runs down approaching the right angle. The diagram of volume flux  $Q'$  shows more predominant difference in magnitude between run-up and run-down phases, because the water depth  $h'$  becomes larger in run-up phase than in run-down phase. This property is more evident as the location  $(x - x_0)/x_0$  ( $x_0 = d'_B/S'$ : the position of still water shoreline) is in the direction of landward. These properties seem to be useful to explain the zig-zag sediment transport in a swash zone. The velocity vector  $v'$  or the volume flux vector  $Q'$  may govern the sediment movement corresponding whether the transport mode is bed load or suspended load, respectively.

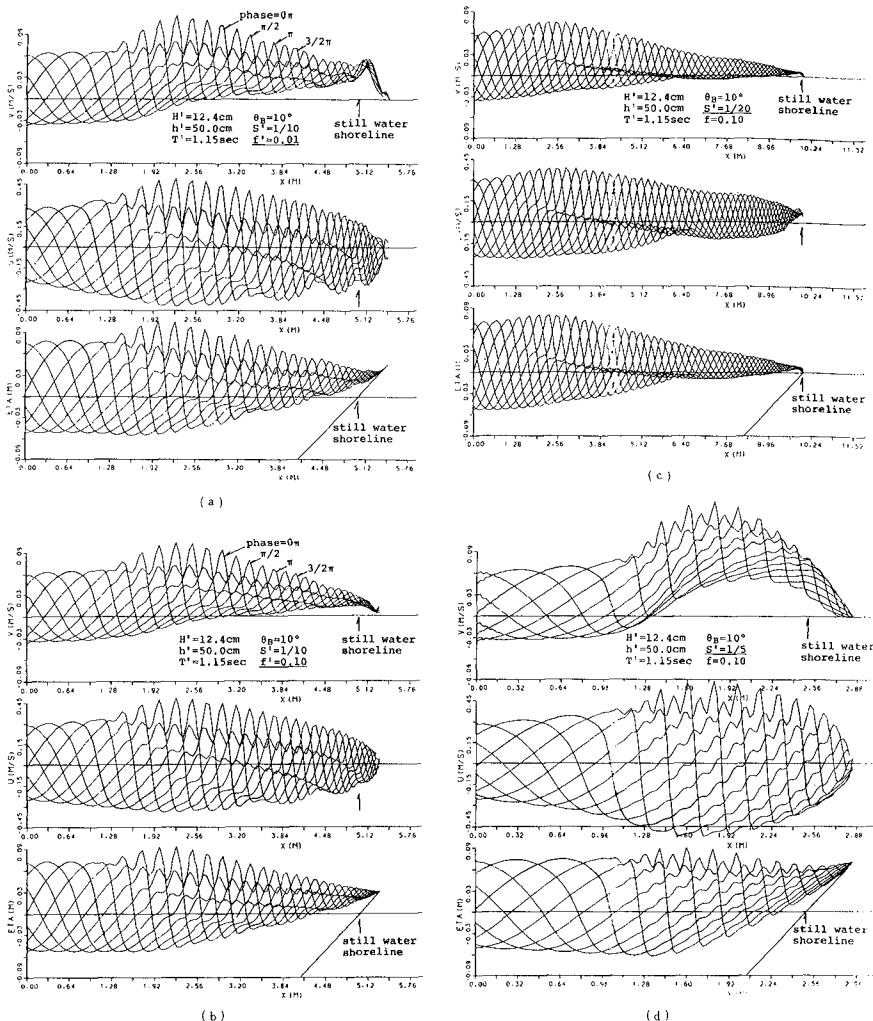


Fig. 2: Spatial variations of longshore velocity  $v'$  (top), on-offshore velocity  $u'$  (middle) and free surface elevation  $\eta'$  (bottom)

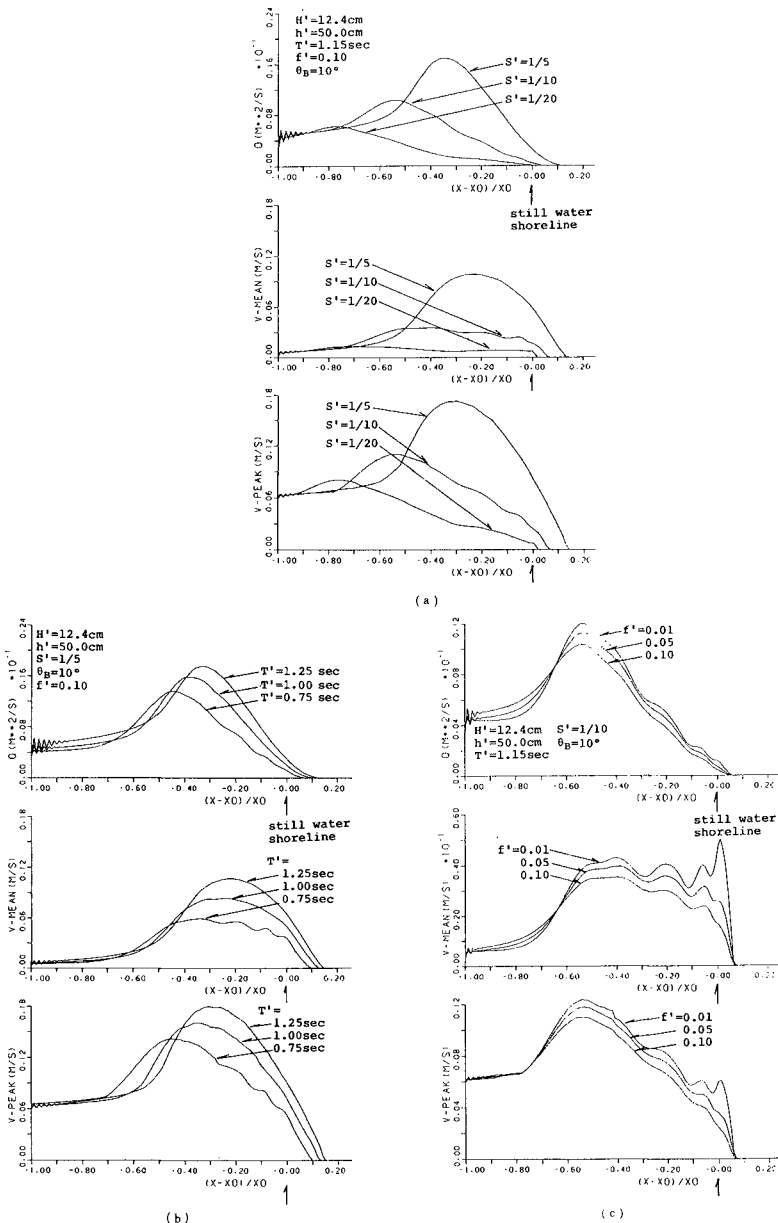


Fig. 3: On-offshore variations of the peak longshore velocity  $v'_{peak}$  (bottom), time averaged longshore velocity  $v'_{mean}$  (middle) and time averaged longshore volume flux  $Q'$  (top)

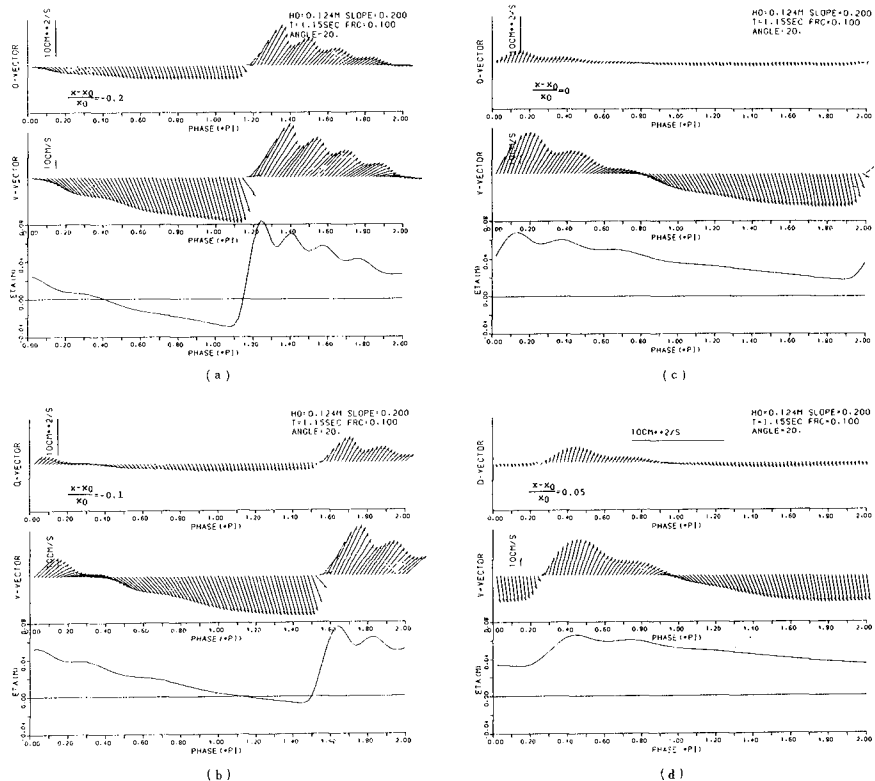


Fig. 4: Temporal variations of free surface elevation  $\eta'$  (bottom), velocity vector  $\mathbf{v}'$  (middle) and longshore volume flux vector  $\mathbf{Q}'$  (top)

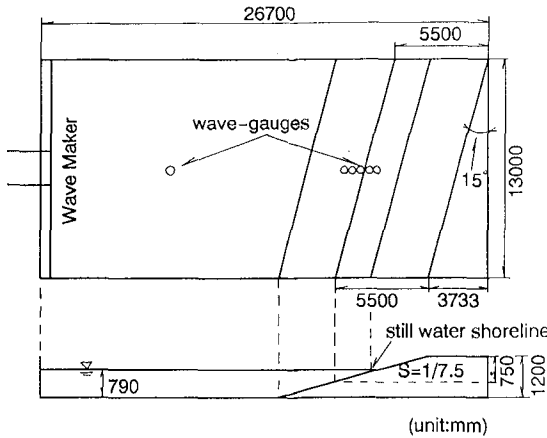


Fig. 5: Wave basin and experimental set-up

### 3. EXPERIMENTAL STUDY

#### 3.1 Experimental Arrangements and Procedure

A wave basin of 26.7m long, 13m wide and 1.2m deep was used. A uniform plane slope of the gradient  $S=1/7.5$  was set up at an angle  $\theta = 15^\circ$  with a wave generator which was equipped at the other end of the basin. The slope was carefully built up by covering 30mm thick concrete mortar with reinforced mesh over a sandy mound. The water depth in the offshore uniform depth region was kept at 79cm constant throughout the experiments. Water surface fluctuations were measured with an array of five capacitance type wave gauges at 12.5cm interval on the slope. The experimental set-up is illustrated as Fig. 5.

In order to measure very shallow flows in a swash zone including landward region of the still water shoreline, tracer method was adopted. An important demand for the tracer is to represent the fluid velocity accurately in the swash zone. Another demand is visibility because the tracer movements were recorded with a bird's-eye video camera locating  $5 \sim 6$  m above the water surface. After several trials, the following three type tracers were chosen: a fluorescent color sphere float of styrene form with 3cm in diameter(type-A), a 2.5mm thick circular plate made of plywood with 110mm diameter(type-B) and a 6.6mm thick octagonal plate made of plywood with 93mm in diagonal length(type-C). A small electro-magnetic current meter with a cylindrical shape sensor 16mm in length and 5mm in diameter was also used in the preliminary measurements.

For each test run, the velocity measurement was started two minutes after the start of wave generation to attain the steady state condition. The velocity measuring area for the tracer method should be chosen where the uniformity of the longshore current is confirmed. In order to detect the position of a moving tracer throughout the surf zone and swash zone, a 20cm-mesh reference

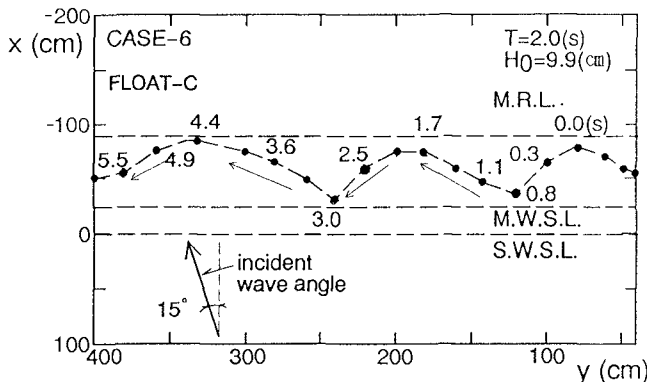


Fig. 6: Trajectories of tracers

frame of  $3.6\text{m} \times 3.6\text{m}$  was installed. The trajectories of the tracers over the reference frame were recorded at an interval of 1/30 second. Frame by frame analysis of the video film yields Lagrangian velocities both in on-offshore and alongshore directions. For the detailed descriptions of the experiment, see Asano et al.(1994).

### 3.2 Experimental Results on Longshore Velocity in Surf and Swash Zone

Fig. 6 shows examples of plane trajectories of tracers. Each tracer runs up obliquely on the slope, then tends to run-down vertically. This property corresponds to the numerical results illustrated in Fig. 4.

The longshore velocity of a fluid particle was herein evaluated from the alongshore displacement of the tracer during one wave cycle. Fig. 7 shows an example of the on-offshore distributions of longshore current velocity  $V$ . In plotting the data  $V$ , the  $x$ -position was determined by the central point of a tracer over one wave cycle. Some data which the position after one wave cycle were clearly shifted in the on-offshore direction were discarded. Fewer data are obtained in the negative  $x$ -region because the plate type tracers (type-B and C) are frequently thrown up on the slope. Also fewer data are available slightly onshore of the breaking point because white-caps generated by breaking waves often make tracer invisible. Since no obvious differences by the tracer types are noticed in Fig. 7, results will be shown without distinguishing the tracer types in the following. One important point in this result is that the longshore current velocity at the still water shoreline  $x=0$  has the same order of magnitude as that in the surf zone.

Fig. 8 shows the results where the incident wave heights are almost the same. Here, the measured longshore current velocities including the case shown in Fig. 7 are averaged over every 10cm segment in the on-offshore direction, then plotted in the non-dimensional form  $V/V_{max}$  against normalized alongshore

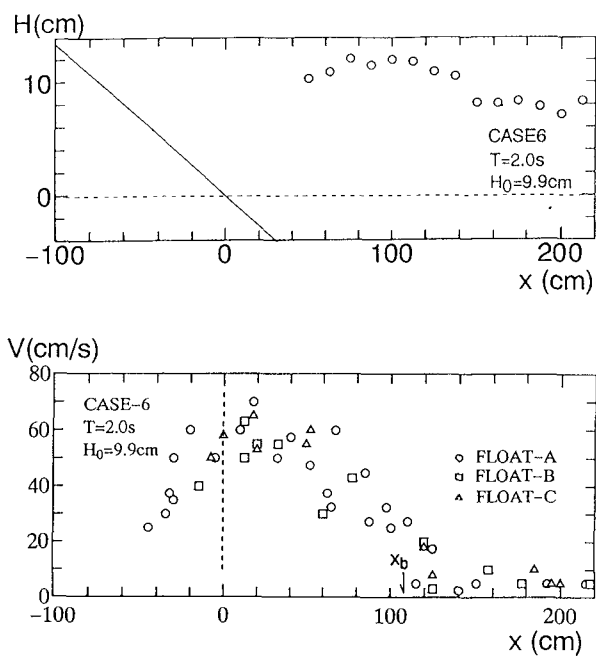


Fig. 7: On-offshore distributions of wave height and longshore current velocity

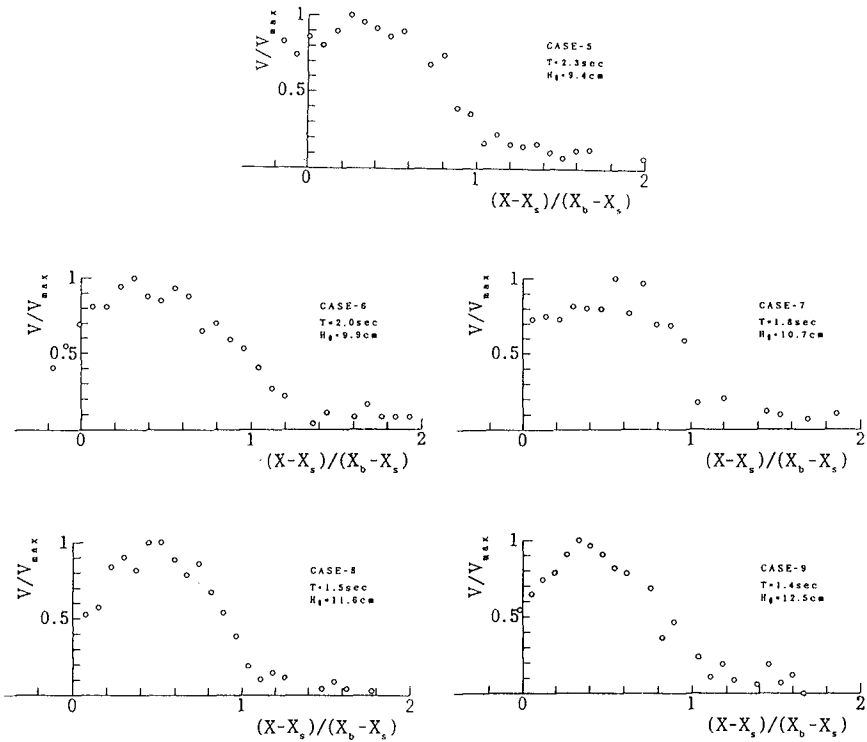


Fig. 8: On-offshore distributions of longshore current velocity

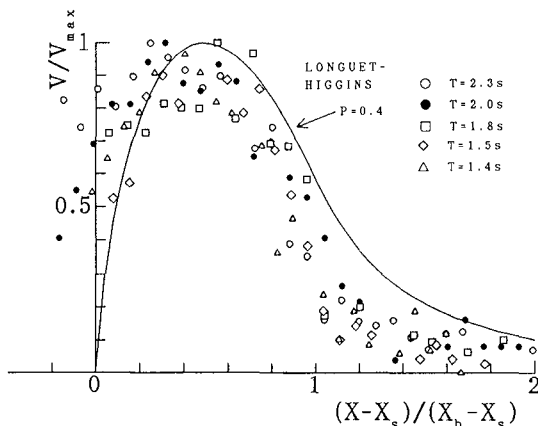


Fig. 9: On-offshore distributions of longshore current velocity and comparison with Longuet-Higgins' (1970) analytical solution

position.

Fig. 9 shows the comparison of all the data shown in Fig. 8 with Longuet-Higgins' (1970) analytical solution, in which the ratio between the horizontal mixing term and the friction term  $P$  is given by 0.4. It should be noted that little attention has been paid on the longshore current velocity at and beyond the shoreline landward, and conventional time averaged models inevitably predict the longshore current at the shoreline  $V_s$  as 0. Whereas, Fig. 8 and Fig. 9 show that  $V_s$  has a substantial value even at the mean water shoreline  $x = x_s$  after wave set-up. It is also noticed that the longshore velocity at the mean water shoreline  $V_s$  increases with the incident wave period. This property agrees with the numerical results shown in Fig. 3 (b).

Further investigation reveals that the present results as well as a part of Visser (1991)'s results on  $V_s/V_{max}$  are well arranged by the surf similarity parameter (See Asano et al. (1994)).

#### 4. CONCLUSIONS

A numerical model is developed to predict the flow characteristics in a swash zone for obliquely incident wave trains. The two dimensional shallow water equations are de-coupled into independent equations each for on-off shore motion and for longshore motion. The numerical results on the longshore velocity in a swash zone are compared with measured results by the tracer method. Both the numerical and experimental studies reveal the following properties.

- (1) Substantial longshore velocities have been obtained even in the landward region of the still water shoreline.
- (2) The magnitude of the longshore current velocities at the mean water shoreline is found to increase with the beach slope and incident wave period.

(3) The swash wave which rushed up obliquely on a slope tend to run down approaching to the right angle with the shoreline. The property may cause zig-zag longshore sediment transport inherent in swash zone.

Quantitative comparison between numerical and experimental results should be conducted with considering the effects of the vertical velocity profiles and turbulence in swash waves.

## REFERENCES

- Asano T., H. Suetomi and J. Hoshikura (1994): Velocity measurements in swash zone generated by obliquely incident waves, Coastal Engineering in Japan (in Printing).
- Asano T. and T. Nakano (1992): Numerical Analysis on obliquely incident run-up waves, Proc. of Coastal Engrg., JSCE, Vol. 39, pp.26-30 (in Japanese).
- Bodge K. R. and R. G. Dean (1987): Short-term impoundment of long-shore transport, Proc. of Coastal Sediment '87, pp.468-483.
- Hibberd, S. and Peregrine, D.H. (1979): Surf and run-up on a beach; A uniform bore, J. of Fluid Mech., Vol.95, pp.323-345.
- Kamphuis J. W. (1991, a): Wave transformation, Coastal Engineering, Vol.15, pp.173-184.
- Kamphuis J. W. (1991, b): Alongshore sediment transport rate distribution, Proc. of Coastal Sediment '91, pp.170-183.
- Kobayashi N., A. K. Otta and I. Roy (1987): Wave reflection and run-up on rough slopes, J. of Waterway, Port, Coastal and Ocean Div., ASCE, Vol.113, No.3, pp.282-298.
- Longuet-Higgins, M. S. (1970) : Longshore current generated by obliquely incident sea waves, J. Geophys. Res. , Vol.75, pp.6778-6801.
- Ryrie S. C. (1983): Longshore motion generated on beaches by obliquely incident bores, J. Fluid Mech., Vol.129, pp.193-212.
- Thornton E. B. and S. Abdelrahman (1991): Sediment transport in the swash due to obliquely incident wind-waves modulated by infragravity waves ; Proc. Coastal Sediment '91, pp. 100-113.
- Visser, P. J.(1991) : Laboratory measurements of uniform longshore currents, Coastal Engineering, Vol. 15, pp.563-593.